HHS Public Access

Author manuscript

Brain Struct Funct. Author manuscript; available in PMC 2017 February 28.

Published in final edited form as:

Brain Struct Funct. 2015 September ; 220(5): 3011–3022. doi:10.1007/s00429-014-0841-6.

Glutamatergic phenotype of glucagon-like peptide 1 neurons in the caudal nucleus of the solitary tract in rats

H. Zheng,

Department of Neuroscience, University of Pittsburgh, A210 Langley Hall, Pittsburgh, PA 15260, USA

R. L. Stornetta,

Department of Pharmacology, University of Virginia, Charlottesville, VA, USA

K. Agassandian, and

Department of Neuroscience, University of Pittsburgh, A210 Langley Hall, Pittsburgh, PA 15260, USA

Linda Rinaman

Department of Neuroscience, University of Pittsburgh, A210 Langley Hall, Pittsburgh, PA 15260, USA

Abstract

The expression of a vesicular glutamate transporter (VGLUT) suffices to assign a glutamatergic phenotype to neurons and other secretory cells. For example, intestinal L cells express VGLUT2 and secrete glutamate along with glucagon-like peptide 1 (GLP1). We hypothesized that GLP1-positive neurons within the caudal (visceral) nucleus of the solitary tract (cNST) also are glutamatergic. To test this, the axonal projections of GLP1 and other neurons within the cNST were labeled in rats via iontophoretic delivery of anterograde tracer. Dual immunofluorescence and confocal microscopy was used to visualize tracer-, GLP1-, and VGLUT2-positive fibers within brainstem, hypothalamic, and limbic forebrain nuclei that receive input from the cNST. Electron microscopy was used to confirm GLP1 and VGLUT2 immunolabeling within the same axon varicosities, and fluorescent in situ hybridization was used to examine VGLUT2 mRNA expression by GLP1-positive neurons. Most anterograde tracer-labeled fibers displayed VGLUT2-positive varicosities, providing new evidence that ascending axonal projections from the cNST are primarily glutamatergic. Virtually all GLP1-positive varicosities also were VGLUT2-positive. Electron microscopy confirmed the colocalization of GLP1 and VGLUT2 immunolabeling in axon terminals that formed asymmetric (excitatory-type) synapses with unlabeled dendrites in the hypothalamus. Finally, in situ hybridization confirmed that GLP1-positive cNST neurons express VGLUT2 mRNA. Thus, hindbrain GLP1 neurons in rats are equipped to store glutamate in synaptic vesicles, and likely co-release both glutamate and GLP1 from axon varicosities and terminals in the hypothalamus and other brain regions.

Correspondence to: Linda Rinaman.

Keywords

Glutamate; VGLUT2; Paraventricular nucleus of the hypothalamus; Bed nucleus of the stria terminals; Electron microscopy; In situ hybridization; Confocal microscopy

Introduction

Vesicular glutamate transporter (VGLUT) is a key membrane component for glutamatergic cellular signaling (Moriyama and Yamamoto 2004; Fremeau et al. 2001). VGLUT is responsible for the vesicular uptake of glutamate, which is essential for exocytosis (Liguz-Lecznar and Skangiel-Kramska 2007). VGLUT belongs to the SLC17/type I phosphate transporter family, and comprises three isoforms, i.e., VGLUT1, VGLUT2, and VGLUT3 (Reimer and Edwards 2004; Liguz-Lecznar and Skangiel-Kramska 2007; Johnson et al. 2004; Varoqui et al. 2002; Schafer et al. 2002). VGLUT expression formally identifies neurons that are primarily glutamatergic, and also suffices to assign a glutamatergic phenotype to neurons and other secretory cells that express and release additional signaling molecules (Moriyama and Yamamoto 2004; El Mestikawy et al. 2011; Herzog et al. 2004; Noh et al. 2010).

A previous study demonstrated VGLUT2 expression by intestinal enteroendocrine L cells that secrete glucagon-like peptide 1 (GLP1) (Hayashi et al. 2003), a gut hormone that also is expressed by a discrete population of caudal brainstem neurons (Larsen et al. 1997a; Han et al. 1986). Results of in vitro studies indicate that clonal L cells store and co-release glutamate and GLP1 via vesicular exocytosis (Uehara et al. 2006), raising the possibility that brainstem GLP1 neurons also use glutamate as a signaling molecule. Somatic GLP1 immunolabeling and expression of preproglucagon mRNA (the gene encoding the protein from which GLP1 is cleaved) are localized to neurons within the caudal (visceral) nucleus of the solitary tract (cNST) and adjacent medullary reticular formation in rodents and primates, including humans (Han et al. 1986; Larsen et al. 1997a, b; Vrang and Grove 2011; Zheng et al. 2014). In rats, hindbrain GLP1 neurons are recruited/activated by stimuli associated with real or perceived homeostatic threats [cf. (Maniscalco et al. 2012; Vrang et al. 2003; Rinaman 1999b)], and give rise to a diffuse network of fibers and terminals that innervate brainstem, hypothalamic, and limbic forebrain regions where GLP1 receptors (GLP1-Rs) are expressed (Maniscalco et al. 2012; Rinaman 1999b; Merchenthaler et al. 1999; Vrang et al. 2007).

VGLUT2 mRNA is abundant in the rodent NST, whereas VGLUT3 mRNA expression is more limited (Schafer et al. 2002), and VGLUT1 mRNA expression is absent (Stornetta et al. 2002a). Ultrastructural evidence indicates that GLP1-positive terminals form asymmetric (i.e., excitatory-type) synaptic contacts with hypothalamic target neurons (Sarkar et al. 2003), consistent with a glutamatergic phenotype. We hypothesized that GLP1 neurons in the rat cNST express VGLUT2 mRNA, similar to GLP1-expressing intestinal L cells (Hayashi et al. 2003). Research indicates that GLP1-R agonists increase glutamatergic signaling within brain regions that receive GLP1 synaptic input (Acuna-Goycolea and van den Pol 2004; Mietlicki-Baase et al. 2013), but the possibility that GLP1 neurons are

themselves glutamatergic has not been subjected to experimental scrutiny. This possibility has important implications for understanding the functional role of GLP1 neurons within central neural circuits that control behavioral, endocrine, and emotional responses to cognitive and interoceptive homeostatic threats (Maniscalco et al. 2012; Kinzig et al. 2003). The present study uses anterograde neural tracing, dual immunofluorescence, confocal and electron microscopy, and in situ hybridization to demonstrate the glutamatergic phenotype of hindbrain GLP1 neurons that innervate brainstem, hypothalamic, and limbic forebrain regions in rats.

Materials and methods

Animals

Adult male Sprague Dawley rats (Harlan Laboratories, Indianapolis, IN; 250–300 g) were singly housed in hanging wire-bottom stainless steel cages in an AAALAC-accredited controlled environment (20–22 °C, 12 h light/dark, lights on at 0700 hours) with ad libitum access to pelleted chow (Purina #5001) and tap water. Rats were acclimated to this environment for at least 1 week before tracer injection surgery, described below ("Anterograde tracer delivery"), or before perfusion without tracer injection. Experimental protocols were approved by the University of Pittsburgh Institutional Animal Care and Use Committee, and are consistent with the U.S. Public Health Service's Policy on Humane Care and Use of Laboratory Animals and the Guide for the Care and Use of Laboratory Animals.

Anterograde tracer delivery

Phaseolus vulgaris leucoagglutinin (PHAL; Vector Laboratories, 2.5 % in 0.1 M phosphate buffer) was delivered unilaterally into the dorsal vagal complex at the rostrocaudal level of the caudal area postrema (AP), approximately 14.2 mm caudal to bregma. Tracer solution was freshly prepared from frozen stocks within 2 h of injection. Rats ($n = 3$) were anesthetized by isoflurane inhalation (Halocarbon Laboratories, River Edge, NJ; 1–3 % in oxygen) and secured in a stereotaxic frame using blunt ear bars, with the head ventroflexed by ~11°. The skin over the dorsal neck surface was shaved, sterilized, incised along the midline, and the neck muscles retracted to expose the atlantooccipital membrane overlying the dorsal surface of the caudal medulla. With the aid of a surgical microscope, the membrane was opened with a sterile needle to reveal obex on the dorsomedial medullary surface, at the caudal tip of the AP. To target tracer delivery into the caudal medial NST, a glass iontophoretic micro-pipette (inner tip diameter ~20 μm) filled with tracer was positioned 0.4 mm lateral to obex, then the tip was advanced 0.4 mm below the medullary surface at a 10° angle from the vertical plane. PHAL was delivered using a 7 s on/off pulsed current of 5 μA for 10 min. The glass pipette was removed 2 min after tracer delivery, the skin incision sutured, and the animal allowed to recover from surgery on a warm pad before being returned to its home cage.

Perfusion fixation and tissue collection for light microscopy

Ten days after iontophoretic delivery of PHAL into the cNST, or after 1 week of laboratory acclimation (for non-tracer ISH and ICC studies), rats were deeply anesthetized with a lethal dose of pentobarbital sodium (Fatal Plus; 100 mg/kg BW, i.p., Butler Schein, Columbus,

OH) and transcardially perfused, first with 100 ml 0.15 M NaCl, then with 150 ml acrolein–paraformaldehyde (PF) mixture [1.5 % acrolein (Polysciences, Inc., Warrington, PA, USA) and 2.0 % PF (Sigma-Aldrich, St. Louis, MO, USA) in 0.1 M phosphate buffer, pH 7.4], followed by 100 ml 2.0 % PF in 0.1 M phosphate buffer. Fixed brains were removed from the skull, blocked, postfixed in 2.0 % PF for 5–6 h at 4 °C, submerged in 20 % sucrose solution for 18–24 h at 4 °C, then sectioned in the coronal plane from the upper cervical spinal cord through the rostral corpus callosum using a freezing stage sliding microtome (Leica). Six series of floating sections (30 or 35 μm thickness) were collected into buffer. Tissue sections were either immediately processed for ICC alone or for ICC after in situ hybridization, or were stored at −20 °C in cryopreservant (1.0 M sucrose, 30.0 % ethylene glycol, and 1.0 % poly-vinylpyrrolidone-40 in 50.0 mM sodium phosphate buffer, pH 7.4) for later use. When obtaining tissues to be processed via ISH + ICC (described below), RNAse-free solutions were used for perfusion, tissue collection, storage, and subsequent processing.

Immunocytochemical (ICC) localization of PHAL, VGLUT2, and GLP1

Dual ICC labeling procedures were carried out at room temperature on a shaker table. Antibodies were diluted in phosphate buffer (PB) containing 0.3 % Triton, 1.0 % goat serum, and 1.0 % donkey serum, and all rinses were in PB (3 × 10 min each). Tissue sections were rinsed, pretreated for 15 min in 1.0 % sodium borohydride, rinsed, incubated for 15 min in 0.2 % hydrogen peroxide, rinsed, then incubated for 22–24 h in a primary antibody cocktail containing either rabbit anti-GLP1 (1:10K, T-4363, Peninsula Laboratories, San Carlos, CA, USA) and mouse anti-VGLUT2 (1:1,000, MAB5504, Millipore, Temecula, CA, USA), or rabbit anti-PHAL (1:1,000, AS-2300, Vector Laboratories, Burlingame, CA, USA) and mouse anti-VGLUT2. To reveal PHAL and VGLUT2, sections were rinsed and incubated 2 h at room temperature followed by 18 h at 4 °C in a secondary antibody cocktail containing Cy3-conjugated donkey anti-rabbit IgG and Alexa488-conjugated donkey anti-mouse IgG (1:300 each, Jackson ImmunoResearch). For GLP1 and VGLUT2, sections were rinsed and incubated 2 h in a secondary antibody cocktail containing HRP-conjugated goat anti-rabbit IgG (1:300, PerkinElmer) and Alexa488-conjugated donkey anti-mouse IgG (1:300, Jackson ImmunoResearch). After PBS rinses, sections were reacted for 10 min with tyramide conjugated to Cy3 (1:300 in amplification diluent, PerkinElmer, Waltham, MA, USA) to reveal GLP1 labeling, then rinsed and mounted onto Superfrost Plus Microscope Slides, allowed to dry, dehydrated and defatted in a series of graded ethanols followed by xylene, and finally coverslipped with Cytoseal 60 mounting medium. Dual immunofluorescent labeling was examined and photographed using a confocal microscope, as described below (see “Confocal imaging”).

As previously reported (Zheng et al. 2014), the specificity of GLP1 immunolabeling was verified by omitting the anti-GLP1 antibody from primary incubation solution, and also using anti-GLP1 antibody that was pre-incubated with a tenfold higher concentration of synthetic GLP1 (7-37) acetate salt (H-9560, Bachem) overnight at room temperature. Both procedures eliminated GLP1 immunolabeling in rat brain tissue sections. The specificity of mouse anti-VGLUT2 has been characterized and reported (Griffin et al. 2010).

Animal perfusion and tissue collection for electron microscopy

Rats to be used for ultrastructural analysis of GLP1 and VGLUT2 immunolabeling ($n = 4$) were anesthetized with an overdose of pentobarbital sodium (i.p.) and then perfused transcardially with phosphate buffered saline (PBS) followed by 100 ml of PBS containing 3.75 % acrolein and 2 % PF, followed by 200 ml of 2 % PF alone. Fixed brains were removed from the skull, postfixed in 2 % PF for 6 h at 4 °C, rinsed for 18–24 h in several changes of PBS, and then sectioned serially in the coronal plane (50 μm) using a vibratome (Technical Products International, Inc., St. Louis, MO, USA). Floating vibratome sections were collected into PBS.

Electron microscopy: pre- and post-embedding immunolabeling of GLP1 and VGLUT2

Coronal vibratome sections through the paraventricular (PVN) and dorsomedial hypothalamic nuclei (DMH) were processed for pre-embedding immunoperoxidase localization of GLP1 using a rabbit polyclonal antibody (T-4363, Lot # 960721-1; Peninsula Laboratories Inc.). Sections were treated with 1 % sodium borohydride in 0.1 M phosphate buffer (PB), rinsed in PB, incubated in 1 % hydrogen peroxide, rinsed again in PB, transferred to cryoprotectant solution, transferred to a −80 °C freezer for 1 h, brought back to room temperature, and then rinsed in 0.1 M Tris-buffered saline (TBS). After 30-min pretreatment in blocking solution (TBS containing 1 % bovine serum albumin, 3 % normal donkey serum, and 0.4 % triton X-100), sections were incubated overnight at room temperature in blocking solution containing rabbit anti-GLP1 (1:7,000). Sections were then rinsed in TBS, incubated in affinity purified biotinylated donkey anti-rabbit IgG (1:250; Jackson ImmunoReseach Laboratories, Inc., West Grove, PA, USA), rinsed, and then processed using Vectastain Elite avidin–biotin reagents (Vector Laboratories; Burlingame, CA). The immunoperoxidase reaction was generated by incubating sections for 10 min in TBS containing 0.05 % diaminobenzidine and 0.01 % hydrogen peroxide.

Immunoperoxidase-reacted vibratome sections were postfixed in 1 % osmium tetroxide for 30 min, washed in repeated changes of 0.1 M PB, and dehydrated in a graded ethanol series. Sections were then passed through multiple changes of acetone followed by sequential changes of increasing concentrations of epon–araldite plastic resin diluted in acetone. After the final change into 100 % resin, sections were flat-embedded between two acrylic sheets and polymerized overnight at 60 °C. GLP1 immunoperoxidase labeling within hypothalamic regions of interest (i.e., the PVN and DMH) was visualized in transilluminated flat-embedded sections. These regions were trimmed from their surrounding section, glued flat onto blank plastic stubs, and then razor-trimmed into a trapezoidal shape containing either the PVN or DMH. Ultrathin floating sections (~600 angstroms) were cut using a Leica Ultracut R ultramicrotome, moved onto formvar-coated thin slot nickel grids, and stored in serial order in grid boxes.

For post-embedding immunogold detection of VGLUT2, ultrathin sections on slot grids were rinsed in TBS, incubated in 5 % bovine serum albumin, and placed into mouse anti-VGLUT2 antibody (1:150) in TBS overnight at 4 °C. Grids were washed in TBS and placed into a 1:10 dilution of colloidal gold donkey anti-mouse IgG (15 nm, EM grade; Aurion) for 1.5 h, rinsed with TBS and then with ddH_2O.

Dual-labeled ultrathin sections were examined and photographed using a transmission electron microscope (Morgagni, FEI, Hillsboro, OR, USA) equipped with a CCD camera (Advanced Microscopy Techniques, Danvers, MA, USA). To facilitate identification of electron-dense GLP1 immunoperoxidase reaction product, sections were not counterstained with heavy metal salts that absorb electrons.

Combined in situ hybridization (ISH) and immunocytochemistry (ICC)

In situ hybridization to localize VGLUT2 mRNA was performed as previously described (Stornetta et al. 2002a, b), with a few modifications. VGLUT2 DNA was amplified from rat brainstem poly-A+ RNA using a one-step RT-PCR (Titan One Tube RT-PCR System; Roche Molecular Biochemicals, Mannheim, Germany). The DNA for VGLUT2 was amplified by using the primers: forward 5′cggggaaagaggggataaag3′ and reverse 5′acacaaagcaga gagggac3′ (Weston et al. 2003), yielding a 3,373 base pair product that was subcloned into the plasmid vector, pCR-TOPO (Invitrogen, Carlsbad, CA, USA). After verifying the identity of the inserted DNA by sequencing, single-stranded RNA was synthesized in an in vitro polymerization reaction using either SP6 or T7 RNA polymerases in the presence of digoxigenin-11-UTP (Roche Molecular Biochemicals). The efficiency of digoxigenin-11-UTP incorporation was estimated by direct immunological detection on dot blots using a sheep polyclonal anti-digoxigenin antibody (Roche Molecular Biochemicals).

VGLUT2 ISH was performed on free-floating coronal tissue sections through the caudal medulla (~14 mm caudal to bregma), where GLP1 neurons are most prevalent. ISH was completed before ICC localization of GLP1 was performed in the same tissue sections. Five to six consecutive coronal tissue sections from each rat ($n = 8$) were rinsed in 0.1 M PBS, pretreated for 15 min with 1.0 % sodium borohydride in PBS, rinsed 30 min with PBS, and then incubated for 15 min in 0.20 % hydrogen peroxide in PBS. Pretreated sections were then placed into prehybridization solution at room temperature for 45 min, then moved to 37 °C for 1 h. The prehybridization mixture contained 0.3 M NaCl, 10.0 mM Tris–Cl (pH 8.0), 1.0 mM ethylenediamine tetraacetic acid (EDTA), 0.5 mg/ml yeast tRNA (AM7119, Life Technologies, Grand Island, NY), 1.0× Denhardt’s solution, 50.0 % deionized formamide, 10.0 % dextran sulfate, and 0.5 mg/ml herring sperm (Sigma-Aldrich). At the end of the 1 h prehybridization period, digoxigenin-labeled VGLUT2 riboprobe (Stornetta et al. 2002a, b) (50–100 pg/μl) was added and sections were hybridized at 55 °C for 22–24 h. Hybridized sections were rinsed sequentially with 4× saline sodium citrate (SSC) containing 10.0 mM sodium thiosulfate, treated with RNase A (20.0 μg/ml, DIAGEN Inc., Valencia, CA, USA), rinsed with RNAse buffer (10.0 mM Tris pH 8.0, 500.0 mM NaCl, 10.0 mM EDTA), and then rinsed in decreasing concentrations of SSC solution. All incubations and rinses were conducted at 37 °C for 30 min, except the final SSC (0.1×) rinse which was conducted at 55 °C for 1 h.

Fluorescence labeling of the digoxigenin-tagged hybridized riboprobe was combined with dual GLP1 immunofluorescence. All rinses (3 × 10 min each in 0.1 M TBS, pH 7.4) and incubations were conducted at room temperature on a rotating platform, unless otherwise noted. Antibodies were diluted in immersion buffer (TBS containing 5 % goat serum, 5 % donkey serum, 2 % bovine serum albumin, and 0.5 % Triton-X 100). Sections were

incubated sequentially for 30 min in immersion buffer, 22–24 h in rabbit anti-GLP1 (1:15K), rinsed, and then incubated in a cocktail containing horseradish peroxidase (HRP)-conjugated goat anti-rabbit IgG (1:300, PerkinElmer, Waltham, MA, USA) and sheep anti-digoxigenin antibody conjugated to alkaline phosphatase (1:1,000, Roche Diagnostics, Indianapolis, IN, USA) for 2 h at room temperature, followed by 18–20 h at 4 °C. GLP1 cell body immunolabeling was revealed by a 10-min reaction in Cy5-conjugated tyramide plus (1:300 in amplification diluent, PerkinElmer, Waltham, MA, USA). For subsequent visualization of VGLUT2 mRNA labeling, sections were incubated for 10 min in detection buffer (0.1 M Tris, 0.1 M NaCl, 0.01 M MgCl; pH 8.0) followed by 2–3 h in HNPP/Fast Red reaction solution (0.1 mg/ml HNPP, 0.1 mg/ml Fast Red in detection buffer, Roche Diagnostics, Indianapolis, IN). The reaction was stopped by three 5 min rinses in PBS–EDTA (0.1 M PBS, 1.0 mM EDTA). To prevent the loss of HNPP/Fast Red reaction precipitation by subsequent mounting media, labeled sections were fixed for 10 min in 4.0 % PF followed by PBS rinses. After a final brief rinse in dH_2O (1–2 min), sections were mounted onto adhesion Superfrost Plus Microscope Slides (Brain Research Laboratories, Waltham, MA, USA), allowed to dry, and quickly defatted with xylene (2 × 5 min). Slides were coverslipped with Cytoseal 60 mounting medium (Fisher Scientific, Pittsburgh, PA, USA) and viewed using a confocal microscope, described below (“Confocal imaging”).

Confocal imaging

Images were obtained using an Olympus BX61/Fluo-view1000 confocal laser scanning microscope in multi-channel mode, and 60× or 100× oil-immersion objectives. Cy3 or Fast Red (in different samples) was excited using the yellow line (559 nm) of the krypton/argon laser, while the green line (488 nm) was used to collect images of Alexa 488-labeled profiles. Cy5 was visualized with the 635 nm laser. For each final 5.0- to 6.0-μm-thick projection image, stacks of ten–fifteen 0.40–0.50-μm-thick optical planes were collapsed. In addition, three-dimensional (3D) rotated images were generated using maximal intensity projections from areas of interest, or from the entire image. Low magnification images (10× or 20×) were acquired using an Olympus BX51 epifluorescence (X-Cite 120) microscope equipped with a Hamamatsu camera. All photographs were imported to Adobe Photoshop (CS 5.1), adjusted for output and threshold to include all information-containing pixels, and adjusted for brightness and contrast to best demonstrate visible fluorescence labeling. No additional photographic alterations were performed.

Results

PHAL anterograde tracing

The anterograde neural tracer PHAL was successfully delivered via iontophoresis in three rats. Tracer delivery resulted in many PHAL-positive neuronal cell bodies located within the cNST at the level of the AP (Fig. 1a), and just caudal to the AP. Tracer delivery included the cNST region where GLP1 neurons are intermingled with dopamine beta hydroxylase (DBH)-positive neurons comprising the caudal A2 noradrenergic (NA) cell group (Fig. 1b). Tracer-labeled cNST neurons gave rise to labeled fibers that occupied brainstem and forebrain regions known to receive input from the cNST, including the parabrachial nucleus, periaqueductal gray, thalamic paraventricular nucleus, hypothalamic paraventricular (PVN),

supraoptic, dorsomedial, and arcuate nuclei, central nucleus of the amygdala, and anterior lateral bed nucleus of the stria terminalis (BNST). The distribution and relative density of anterogradely labeled fibers across brain regions were consistent with previous reports, as recently reviewed (Rinaman 2010, 2011). Confocal images of PHAL-labeled fibers within the PVN and BNST are shown in Figs. 2b and 3b, respectively.

Colocalization of VGLUT2 with PHAL and GLP1

Confocal microscopy revealed that VGLUT2 immunofluorescence was colocalized with anterogradely transported PHAL or with GLP1 immunolabeling in axon varicosities located in every brain region examined, i.e., regions that contained PHAL and/or GLP1 immunolabeling. Although PHAL- or GLP1-positive fiber segments often were VGLUT2-negative (e.g., see Figs. 2b, 3b), individual PHAL- or GLP1-positive fibers could usually be followed through the section to locations where double-labeled, VGLUT2-positive varicose swellings emerged (e.g., see boxed regions in Figs. 2b, 3b, 4a). Three-dimensional, 6-μm-thick Z-stack images from the PVN (Fig. 2), BNST (Fig. 3), cNST (Fig. 4), and other brain regions (not shown, but including the pontine parabrachial nucleus, arcuate and dorsomedial hypothalamic nuclei, and ventral tegmental area) were created using Olympus imaging software included in the FV1000D Laser Confocal Scanning Microscope system software package. 3D images from each region were digitally rotated to confirm extensive colocalization of VGLUT2 with either PHAL or GLP1 immunofluorescence in the same varicose profiles, rather than within distinct profiles that simply overlapped within the tissue section.

Electron microscopy

Many axonal fibers, varicosities, and axon terminals within the hypothalamic PVN and DMH contained floccular, electron-dense GLP1 immunoperoxidase labeling (Fig. 5). As expected, given the absence of GLP1-expressing neurons within the hypothalamus, immunoperoxidase-positive cell bodies or dendrites were not observed. The pre-embedding GLP1 immunoperoxidase reaction product densely filled labeled profiles located near the surface of the vibratome section (e.g., Fig. 5a). GLP1-positive profiles located farther from the surface displayed less dense immunoperoxidase labeling, but typically displayed better preservation of ultrastructure. Particulate VGLUT2 immunogold labeling was similarly prevalent regardless of distance from the surface of the vibratome section, as would be expected for post-embedding labeling. GLP1-positive varicosities often were observed in close apposition to unlabeled dendrites and axon varicosities, with no clear synaptic specializations (Fig. 5a, b). However, despite the lack of heavy metal counterstaining, there was no difficulty identifying many GLP1-positive axon terminals forming asymmetric (i.e., excitatory-type) synaptic contacts with unlabeled dendrites in both the PVN and DMH (Fig. 5c–f). Of approximately 100 GLP1-positive varicosities and synaptic terminals that were photographed within the PVN and DMH, the majority (67) also displayed three or more VGLUT2 immunogold particles (Fig. 5a–f).

In situ hybridization

Consistent with previous reports, VGLUT2 mRNA was expressed by many neurons within the cNST (Stornetta et al. 2002a, b). The present study used the same digoxigenin-labeled

mRNA probe for fluorescent in situ hybridization localization of VGLUT2 mRNA, combined with dual immunofluorescence labeling for GLP1. Confocal microscopy confirmed that all (100 %) GLP1-positive neurons observed within the cNST were double-labeled for VGLUT2 mRNA, as evident in digitally flattened Z-stack and 3D rotated images (Fig. 4b). As expected, many VGLUT2 mRNA-positive neurons within the cNST were GLP1 negative (Fig. 4b).

Discussion

Glucagon-like peptide 1 neurons within the cNST in rats are recruited/activated by stressors that present real or perceived challenges to homeostasis (Maniscalco et al. 2012; Rinaman 1999b; Vrang et al. 2003). Consistent with this, behavioral and physiological responses to centrally administered GLP1 include pituitary stress hormone release, autonomic responses, hypophagia, and anxiety-like behavior (Maniscalco et al. 2012; Kinzig et al. 2003; Donahey et al. 1998; Gulpinar et al. 2000; Larsen et al. 1997b; Mietlicki-Baase et al. 2013; Moller et al. 2002; Nakade et al. 2006, 2007; Rinaman 1999a; Schick et al. 2003; Seeley et al. 2000; Thiele et al. 1998; Turton et al. 1996). A suggested role for central GLP1-R signaling pathways in body energy balance (Tang-Christensen et al. 2001; Hayes 2012; Meeran et al. 1999; vanDijk and Thiele 1999) also is supported by evidence in rats and mice implicating central GLP1 in temperature regulation (Rinaman and Comer 2000; O'Shea et al. 1996) and glucose homeostasis (Sandoval et al. 2008). GLP1-R agonists enhance both excitatory and inhibitory synaptic inputs to identified neurons through presynaptic stimulation of transmitter release from axon terminals (Wan et al. 2007; Acuna-Goycolea and van den Pol 2004), and postsynaptic effects of GLP1 on neuronal activity also are reported (Acuna-Goycolea and van den Pol 2004; Riediger et al. 2010; Hayes 2012). Neuroanatomical results from the present study significantly expand current knowledge regarding the signaling capacity of GLP1 neurons by demonstrating that these neurons are glutamatergic, at least in rats, similar to other neuronal populations that use glutamate as a co-transmitter and/or as a synergistic enhancer of vesicular packaging and release (El Mestikawy et al. 2011).

The extrinsic sources of glutamatergic input to the hypothalamus and limbic forebrain, including the DMH, PVN and anterior lateral BNST, are not completely established (Crestani et al. 2013; Myers et al. 2013; Ulrich-Lai et al. 2011; Ziegler et al. 2012). In the present study, most anterograde tracer-labeled fibers originating from the cNST displayed varicosities that were VGLUT2-positive. These results provide new evidence that ascending neural projections from the cNST to the DMH, PVN, BNST, and other brainstem and forebrain targets are primarily glutamatergic. Since noradrenergic A2 neurons and GLP1 neurons together provide the bulk of ascending projections from the cNST to higher brain regions (Rinaman 2010; Sawchenko and Swanson 1982), the presence of VGLUT2 immunolabeling in nerve terminals arising from the cNST confirms and extends previous findings that A2 neurons express VGLUT2 mRNA in rats (Stornetta et al. 2002a). Further, virtually all GLP1-positive axon varicosities were VGLUT2-positive. Although triple-immunolabeling was not performed, the convergent evidence from this study supports the conclusion that axonal projections arising from GLP1 neurons within the cNST are glutamatergic. Electron microscopic analysis of tissue samples from the hypothalamic PVN and DMH confirmed the colocalization of GLP1 and VGLUT2 immunolabeling in axon

terminals that formed asymmetric (excitatory-type) synapses with unlabeled dendrites. Finally, fluorescent in situ hybridization confirmed that GLP1-positive neurons within the cNST express VGLUT2 mRNA. Thus, hindbrain GLP1 neurons in rats are equipped to store glutamate in synaptic vesicles, and likely co-release both glutamate and GLP1 from their axon varicosities and terminals within the hypothalamus and other brain regions.

Ample evidence suggests that presynaptic signaling codes that promote the release of small molecule (i.e., glutamate) vs. neuropeptide transmitters (i.e., GLP1) may be different [cf. (Schone and Burdakov 2012)]. Speculatively, co-release of GLP1 and glutamate may expand the dynamic range of neuronal signaling by allowing glutamate to be released without GLP1 during brief or low levels of neural activity, whereas GLP1 release may serve to maintain transmission or exert other signaling cascade effects (Hayes 2012) when prolonged stimulation depletes the supply of releasable glutamate [cf. (Schone and Burdakov 2012)]. This could facilitate the ability of GLP1 neurons to participate in ongoing central control of ingestive behavior, stress responses, and emotional responses to internal and external stimuli that require prolonged neural activity.

VGLUT2 is expressed primarily in phylogenetically older CNS regions (i.e., spinal cord, brainstem and hypothalamus), including genetically “hard wired” sensory and visceral-related pathways that display high-fidelity neuro-transmission (Varoqui et al. 2002; Todd et al. 2003). A previous study failed to demonstrate significant colocalization of VGLUT2 mRNA expression by PVN-projecting hindbrain neurons (Ziegler et al. 2012). However, as the study’s authors pointed out, surprisingly few cNST were retrogradely labeled after iontophoretic delivery of FluoroGold neural tracer into the PVN, which precluded meaningful assessment of potential VGLUT2 mRNA expression by PVN-projecting cNST neurons. The hypothalamic PVN and DMH are major axonal targets of hindbrain GLP1 neurons (Maniscalco et al. 2012; Rinaman 1999b; Larsen et al. 1997a; Vrang et al. 2007), and glutamatergic inputs to both hypothalamic nuclei predominantly express VGLUT2 rather than VGLUT1 (Kaneko et al. 2002; Ziegler et al. 2002, 2005). VGLUT2 induction by excitation–transcription coupling leads to increased glutamatergic transmission as part of a coordinated program of Ca^{2+}-mediated signal transcription, potentially contributing to homeostatic synaptic plasticity subsequent to prolonged neuronal activity (Doyle et al. 2010). Indeed, a chronic variable stress paradigm that increases central excitability of the neuroendocrine hypothalamic–pituitary–adrenal (HPA) stress axis has been shown to increase the density of VGLUT2-immunopositive axon terminals within parvocellular (i.e., hypophysiotropic) PVN subregions (Flak et al. 2009). Increased VGLUT2-positive inputs could reflect stress-induced plasticity of glutamatergic signaling by GLP1 neurons, which are known to synapse directly onto corticotropin-releasing hormone-positive PVN neurons at the apex of the HPA axis (Sarkar et al. 2003). Similar effects might be observed within the DMH, anterior ventral BNST, and other central targets of GLP1 axonal input.

To summarize, evidence gathered in this study provides strong neuroanatomical support for the conclusion that GLP1 neurons within the cNST provide glutamatergic input to the PVN and other hypothalamic, brainstem, and limbic forebrain regions. Although the functional significance of GLP1 peptidergic/glutamatergic cotransmission is not yet clear, the results

suggest potential flexibility in neural signaling from the cNST to brain regions involved in behavioral and physiological responses to stressful and emotionally evocative events.

References

Acuna-Goycolea C, van den Pol A. Glucagon-like peptide 1 excites hypocretin/orexin neurons by direct and indirect mechanisms: implications for viscera-mediated arousal. J Neurosci. 2004; 24(37):8141–8152. DOI: 10.1523/JNEUROSCI.1607-04.2004 [PubMed: 15371515]

Crestani CC, Alves FH, Gomes FV, Resstel LB, Correa FM, Herman JP. Mechanisms in the bed nucleus of the stria terminalis involved in control of autonomic and neuroendocrine functions: a review. Curr Neuropharmacol. 2013; 11(2):141–159. DOI: 10.2174/1570159X11311020002 [PubMed: 23997750]

Donahey JC, van Dijk G, Woods SC, Seeley RJ. Intraventricular GLP-1 reduces short- but not long-term food intake or body weight in lean and obese rats. Brain Res. 1998; 779(1–2):75–83. [PubMed: 9473596]

Doyle S, Pyndiah S, De Gois S, Erickson JD. Excitation-transcription coupling via calcium/calmodulin-dependent protein kinase/ERK1/2 signaling mediates the coordinate induction of VGLUT2 and Narp triggered by a prolonged increase in glutamatergic synaptic activity. J Biol Chem. 2010; 285(19):14366–14376. DOI: 10.1074/jbc.M109.080069 [PubMed: 20212045]

El Mestikawy S, Wallen-Mackenzie A, Fortin GM, Descarries L, Trudeau LE. From glutamate co-release to vesicular synergy: vesicular glutamate transporters. Nat Rev Neurosci. 2011; 12(4):204–216. DOI: 10.1038/nrn2969 [PubMed: 21415847]

Flak JN, Ostrander MM, Tasker JG, Herman JP. Chronic stress-induced neurotransmitter plasticity in the PVN. J Comp Neurol. 2009; 517(2):156–165. DOI: 10.1002/cne.22142 [PubMed: 19731312]

Fremeau RT Jr, Troyer MD, Pahner I, Nygaard GO, Tran CH, Reimer RJ, Bellocchio EE, Fortin D, Storm-Mathisen J, Edwards RH. The expression of vesicular glutamate transporters defines two classes of excitatory synapse. Neuron. 2001; 31(2):247–260. [PubMed: 11502256]

Griffin GD, Ferri-Kolwicz SL, Reyes BA, Van Bockstaele EJ, Flanagan-Cato LM. Ovarian hormone-induced reorganization of oxytocin-labeled dendrites and synapses lateral to the hypothalamic ventromedial nucleus in female rats. J Comp Neurol. 2010; 518(22):4531–4545. DOI: 10.1002/cne.22470 [PubMed: 20886620]

Gulpinar MA, Bozkurt A, Coskun T, Ulusoy NB, Yegen BC. Glucagon-like peptide (GLP-1) is involved in the central modulation of fecal output in rats. Am J Physiol Gastrointest Liver Physiol. 2000; 278:G924–G929. [PubMed: 10859222]

Han VK, Hynes MA, Jin C, Towle AC, Lauder JM, Lund PK. Cellular localization of proglucagon/glucagon-like peptide I messenger RNAs in rat brain. J Neurosci Res. 1986; 16(1):97–107. DOI: 10.1002/jnr.490160110 [PubMed: 2427741]

Hayashi M, Morimoto R, Yamamoto A, Moriyama Y. Expression and localization of vesicular glutamate transporters in pancreatic islets, upper gastrointestinal tract, and testis. J Histochem Cytochem. 2003; 51(10):1375–1390. [PubMed: 14500705]

Hayes MR. Neuronal and intracellular signaling pathways mediating GLP-1 energy balance and glycemic effects. Physiol Behav. 2012; 106(3):413–416. DOI: 10.1016/j.physbeh.2012.02.017 [PubMed: 22366059]

Herzog E, Gilchrist J, Gras C, Muzerelle A, Ravassard P, Giros B, Gaspar P, El Mestikawy S. Localization of VGLUT3, the vesicular glutamate transporter type 3, in the rat brain. Neuroscience. 2004; 123(4):983–1002. [PubMed: 14751290]

Johnson J, Sherry DM, Liu X, Fremeau RT Jr, Seal RP, Edwards RH, Copenhagen DR. Vesicular glutamate transporter 3 expression identifies glutamatergic amacrine cells in the rodent retina. J Comp Neurol. 2004; 477(4):386–398. DOI: 10.1002/cne.20250 [PubMed: 15329888]

Kaneko T, Fujiyama F, Hioki H. Immunohistochemical localization of candidates for vesicular glutamate transporters in the rat brain. J Comp Neurol. 2002; 444(1):39–62. [PubMed: 11835181]

Kinzig KP, D'Alessio DA, Herman JP, Sakai RR, Vahl TP, Figueiredo HF, Murphy EK, Seeley RJ. CNS glucagon-like peptide-1 receptors mediate endocrine and anxiety responses to interoceptive and psychogenic stressors. J Neurosci. 2003; 23(15):6163–6170. [PubMed: 12867498]

Larsen PJ, Tang-Christensen M, Holst JJ, Orskov C. Distribution of glucagon-like peptide-1 and other preproglucagon-derived peptides in rat hypothalamus and brainstem. Neuroscience. 1997a; 77(1): 257–270. [PubMed: 9044391]

Larsen PJ, Tang-Christensen M, Jessop DS. Central administration of glucagon-like peptide-1 activates hypothalamic neuroendocrine neurons in the rat. Endocrinology. 1997b; 138(10):4445–4455. [PubMed: 9322962]

Liguz-Lecznar M, Skangiel-Kramska J. Vesicular glutamate transporters (VGLUTs): the three musketeers of glutamatergic system. Acta Neurobiol Exp (Wars). 2007; 67(3):207–218. [PubMed: 17957901]

Maniscalco JW, Kreisler AD, Rinaman L. Satiation and stress-induced hypophagia: examining the role of hindbrain neurons expressing prolactin-releasing peptide or glucagon-like peptide 1. Front Neurosci. 2012; 6:199.doi: 10.3389/fnins.2012.00199 [PubMed: 23346044]

Meeran K, O'Shea D, Edwards CMB, Turton MD, Heath MM, Gunn I, Abusnana S, Rossi M, Small CJ, Goldstone AP, Taylor GM, Sunter D, Steere J, Choi SJ, Ghatei MA, Bloom SR. Repeated intracerebroventricular administration of glucagon-like peptide-1-(7-26) amide or exendin-(9-39) alters body weight in the rat. Endocrinology. 1999; 140(1):244–250.

Merchenthaler I, Lane M, Shughrue P. Distribution of pre-proglucagon and glucagon-like peptide-1 receptor messenger RNAs in the rat central nervous system. J Comp Neurol. 1999; 403(2):261–280. [PubMed: 9886047]

Mietlicki-Baase EG, Ortinski PI, Rupprecht LE, Olivos DR, Alhadeff AL, Pierce RC, Hayes MR. The food intake-suppressive effects of glucagon-like peptide-1 receptor signaling in the ventral tegmental area are mediated by AMPA/kainate receptors. Am J Physiol Endocrinol Metab. 2013; 305(11):E1367–E1374. DOI: 10.1152/ajpendo.00413.2013 [PubMed: 24105414]

Moller C, Sommer W, Thorsell A, Rimondini R, Heilig M. Anxiogenic-like action of centrally administered glucagon-like peptide-1 in a punished drinking test. Prog Neuropsychopharmacol Bol Psychiatry. 2002; 26(1):119–122.

Moriyama Y, Yamamoto A. Glutamatergic chemical transmission: look! Here, there, and anywhere. J Biochem. 2004; 135(2):155–163. [PubMed: 15047716]

Myers B, Mark Dolgas C, Kasckow J, Cullinan WE, Herman JP. Central stress-integrative circuits: forebrain glutamatergic and GABAergic projections to the dorsomedial hypothalamus, medial preoptic area, and bed nucleus of the stria terminalis. Brain Struct Funct. 2013; doi: 10.1007/s00429-013-0566-y

Nakade Y, Tsukamoto K, Pappas TN, Takahashi T. Central glucagon-like peptide 1 delays solid gastric emptying via central CRF and peripheral sympathetic pathways in rats. Brain Res. 2006; 1111:117–121. [PubMed: 16884700]

Nakade Y, Tsukamoto K, Iwa M, Pappas TN, Takahashi T. Glucagon-like peptide 1 accelerates colonic transit via central CRF and peripheral vagal pathways in conscious rats. Auton Neurosci. 2007; 131(1–2):50–56. [PubMed: 16938493]

Noh J, Seal RP, Garver JA, Edwards RH, Kandler K. Glutamate co-release at GABA/glycinergic synapses is crucial for the refinement of an inhibitory map. Nat Neurosci. 2010; 13(2):232–238. DOI: 10.1038/nn.2478 [PubMed: 20081852]

O'Shea D, Gunn I, Chen X, Bloom S, Herbert J. A role for central glucagon-like peptide-1 in temperature regulation. Neuroreport. 1996; 7:830–832. [PubMed: 8733755]

Reimer R, Edwards R. Organic anion transport is the primary function of the SLC17/type I phosphate transporter family. Pflugers Arch Gesamte Physiol Menschen Tiere. 2004; 447(5):629–635. [PubMed: 12811560]

Riediger T, Eisele N, Scheel C, Lutz TA. Effects of glucagon-like peptide 1 and oxyntomodulin on neuronal activity of ghrelin-sensitive neurons in the hypothalamic arcuate nucleus. Am J Physiol Regul Integr Comp Physiol. 2010; 298(4):R1061–R1067. DOI: 10.1152/ajpregu.00438.2009 [PubMed: 20147608]

Rinaman L. A functional role for central glucagon-like peptide-1 receptors in lithium chloride-induced anorexia. Am J Physiol. 1999a; 277:R1537–R1540. [PubMed: 10564228]

Rinaman L. Interoceptive stress activates glucagon-like peptide-1 neurons that project to the hypothalamus. Am J Physiol. 1999b; 277:R582–R590. [PubMed: 10444567]

Rinaman L. Ascending projections from the caudal visceral nucleus of the solitary tract to brain regions involved in food intake and energy expenditure. Brain Res. 2010; 1350:18–34. [PubMed: 20353764]

Rinaman L. Hindbrain noradrenergic A2 neurons: diverse roles in autonomic, endocrine, cognitive, and behavioral functions. Am J Physiol Regul Integr Comp Physiol. 2011; 300(2):R222–R235. DOI: 10.1152/ajpregu.00556.2010 [PubMed: 20962208]

Rinaman L, Comer J. Antagonism of central glucagon-like peptide-1 receptors enhances lipopolysaccharide-induced fever. Auton Neurosci Basic Clin. 2000; 85:98–101.

Sandoval DA, Bagnol D, Woods SC, D'Alessio DA, Seeley RJ. Arcuate glucagon-like peptide 1 receptors regulate glucose homeostasis but not food intake. Diabetes. 2008; 57:2046–2054. [PubMed: 18487451]

Sarkar S, Fekete C, Legradi G, Lechan RM. Glucagon-like peptide-1 (7-36) amide (GLP-1) nerve terminals densely innervate corticotropin-releasing hormone neurons in the hypothalamic paraventricular nucleus. Brain Res. 2003; 985:163–168. [PubMed: 12967720]

Sawchenko PE, Swanson LW. The organization of noradrenergic pathways from the brainstem to the paraventricular and supraoptic nuclei in the rat. Brain Res Rev. 1982; 4:275–325.

Schafer MK, Varoqui H, Defamie N, Weihe E, Erickson JD. Molecular cloning and functional identification of mouse vesicular glutamate transporter 3 and its expression in subsets of novel excitatory neurons. J Biol Chem. 2002; 277(52):50734–50748. DOI: 10.1074/jbc.M206738200 [PubMed: 12384506]

Schick RR, Zimmermann JP, Walde TV, Schusdziarra V. Glucagon-like peptide 1-(7-36) amide acts at lateral and medial hypothalamic sites to suppress feeding in rats. Am J Physiol Regul Integr Comp Physiol. 2003; 284:R1427–R1435. [PubMed: 12776726]

Schone C, Burdakov D. Glutamate and GABA as rapid effectors of hypothalamic "peptidergic" neurons. Front Behav Neurosci. 2012; 6:81.doi: 10.3389/fnbeh.2012.00081 [PubMed: 23189047]

Seeley RJ, Blake K, Rushing PA, Benoit S, Eng J, Woods SC, D'Alessio D. The role of CNS glucagon-like peptide-1 (7-36) amide receptors in mediating the visceral illness effects of lithium chloride. J Neurosci. 2000; 20(4):1616–1621. [PubMed: 10662851]

Stornetta RL, Sevigny CP, Guyenet PG. Vesicular glutamate transporter DNPI/VGLUT2 mRNA is present in C1 and several other groups of brainstem catecholaminergic neurons. J Comp Neurol. 2002a; 444(3):191–206. [PubMed: 11840474]

Stornetta RL, Sevigny CP, Schreihofer AM, Rosin DL, Guyenet PG. Vesicular glutamate transporter DNPI/VGLUT2 is expressed by both C1 adrenergic and nonaminergic presympathetic vasomotor neurons of the rat medulla. J Comp Neurol. 2002b; 444:207–220. [PubMed: 11840475]

Tang-Christensen M, Vrang N, Larsen PJ. Glucagon-like peptide containing pathways in the regulation of feeding behaviour. Int J Obes. 2001; 25(suppl 5):S42–S47.

Thiele TE, Seeley RJ, D'Alessio D, Eng J, Bernstein IL, Woods SC, van Dijk G. Central infusion of glucagon-like peptide-1-(7-36) amide (GLP-1) receptor antagonist attenuates lithium chloride-induced c-Fos induction in rat brainstem. Brain Res. 1998; 801(1–2):164–170. [PubMed: 9729361]

Todd AJ, Hughes DI, Polgar E, Nagy GG, Mackie M, Ottersen OP, Maxwell DJ. The expression of vesicular glutamate transporters VGLUT1 and VGLUT2 in neurochemically defined axonal populations in the rat spinal cord with emphasis on the dorsal horn. Eur J Neurosci. 2003; 17(1): 13–27. [PubMed: 12534965]

Turton MD, O'Shea D, Gunn I, Beak SA, Edwards CM, Meeran K, Choi SJ, Taylor GM, Heath MM, Lambert PD, Wilding JP, Smith DM, Ghatei MA, Herbert J, Bloom SR. A role for glucagon-like peptide-1 in the central regulation of feeding. Nature. 1996; 379(6560):69–72. [PubMed: 8538742]

Uehara S, Jung SK, Morimoto R, Arioka S, Miyaji T, Juge N, Hiasa M, Shimizu K, Ishimura A, Otsuka M, Yamamoto A, Maechler P, Moriyama Y. Vesicular storage and secretion of L-glutamate from glucagon-like peptide 1-secreting clonal intestinal L cells. J Neurochem. 2006; 96(2):550–560. DOI: 10.1111/j.1471-4159.2005.03575.x [PubMed: 16336630]

Ulrich-Lai YM, Jones KR, Ziegler DR, Cullinan WE, Herman JP. Forebrain origins of glutamatergic innervation to the rat paraventricular nucleus of the hypothalamus: differential inputs to the

anterior versus posterior subregions. J Comp Neurol. 2011; 519(7):1301–1319. DOI: 10.1002/cne.22571 [PubMed: 21452198]

van Dijk G, Thiele TE. Glucagon-like peptide-1 (7-36) amide: a central regulator of satiety and interoceptive stress. Neuropeptides. 1999; 33(3):406–414. [PubMed: 10657518]

Varoqui H, Schafer MK, Zhu H, Weihe E, Erickson JD. Identification of the differentiation-associated Na +/PI transporter as a novel vesicular glutamate transporter expressed in a distinct set of glutamatergic synapses. J Neurosci. 2002; 22(1):142–155. [PubMed: 11756497]

Vrang N, Grove K. The brainstem preproglucagon system in a non-human primate (Macaca mulatta). Brain Res. 2011; 1397:28–37. DOI: 10.1016/j.brainres.2011.05.002 [PubMed: 21612769]

Vrang N, Phifer CB, Corkern MM, Berthoud HR. Gastric distension induces c-Fos in medullary GLP-1/2-containing neurons. Am J Physiol Regul Integr Comp Physiol. 2003; 285(2):R470–R478. DOI: 10.1152/ajpregu.00732.2002 [PubMed: 12714357]

Vrang N, Hansen M, Larsen PJ, Tang-Christensen M. Characterization of brainstem preproglucagon projections to the paraventricular and dorsomedial hypothalamic nuclei. Brain Res. 2007; 1149:118–126. [PubMed: 17433266]

Wan S, Browning KN, Travagli RA. Glucagon-like peptide-1 modulates synaptic transmission to identified pancreas-projecting vagal motoneurons. Peptides. 2007; 28(11):2184–2191. [PubMed: 17889966]

Weston M, Wang H, Stornetta RL, Sevigny CP, Guyenet PG. Fos expression by glutamatergic neurons of the solitary tract nucleus after phenylephrine-induced hypertension in rats. J Comp Neurol. 2003; 460(4):525–541. DOI: 10.1002/cne.10663 [PubMed: 12717712]

Zheng H, Cai L, Rinaman L. Distribution of glucagon-like peptide 1-immunopositive neurons in human caudal medulla. Brain Struct Funct. 2014; doi: 10.1007/s00429-014-0714-z

Ziegler DR, Cullinan WE, Herman JP. Distribution of vesicular glutamate transporter mRNA in rat hypothalamus. J Comp Neurol. 2002; 448(3):217–229. DOI: 10.1002/cne.10257 [PubMed: 12115705]

Ziegler DR, Cullinan WE, Herman JP. Organization and regulation of paraventricular nucleus glutamate signaling systems: *N*-methyl-D-aspartate receptors. J Comp Neurol. 2005; 484(1):43–56. DOI: 10.1002/cne.20445 [PubMed: 15717303]

Ziegler DR, Edwards MR, Ulrich-Lai YM, Herman JP, Cullinan WE. Brainstem origins of glutamatergic innervation of the rat hypothalamic paraventricular nucleus. J Comp Neurol. 2012; 520(11):2369–2394. DOI: 10.1002/cne.23043 [PubMed: 22247025]

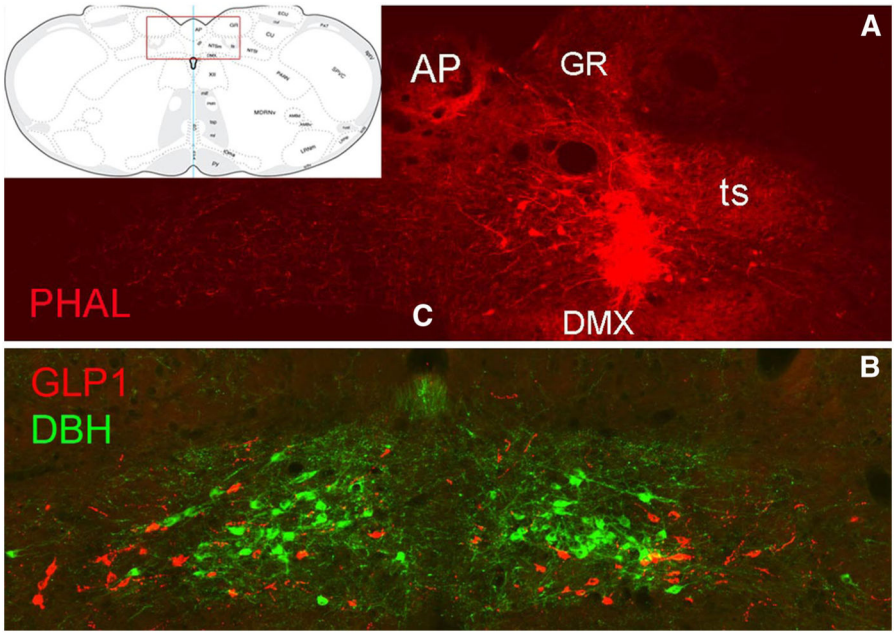

Fig. 1.

PHAL tracer delivery site within the cNST. The *inset* at *upper left* shows the approximate rostrocaudal level targeted (~14.2 mm caudal to bregma), and the *boxed region* corresponds to the photographic images shown in **a**, **b. a** A PHAL tracer delivery site (*red*) centered in the cNST, just dorsal to the DMX. **b** An adjacent tissue section immunolabeled for GLP1 (*red* neurons) and DBH (*green* neurons) to illustrate the locations of intermingling but separate populations of GLP1 and A2 noradrenergic neurons. *AP* area postrema, *c* central canal, *DBH* dopamine beta hydroxylase, *DMX* dorsal motor nucleus of the vagus, *GR* gracile nucleus, *PHAL* phaseolus vulgaris leucoagglutinin, *ts* tractus solitarius

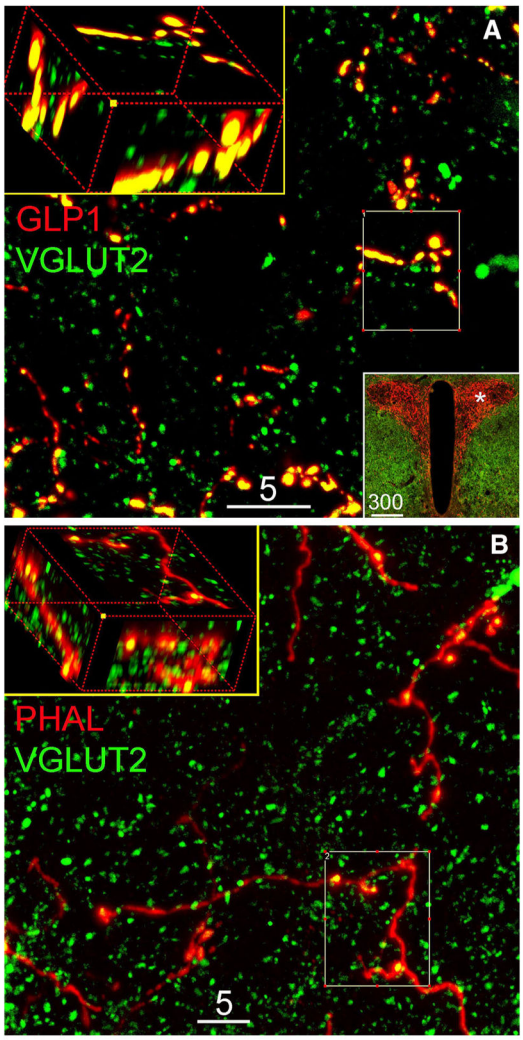

Fig. 2.

Representative confocal images of dual immunofluorescent labeling of **a** VGLUT2 and GLP1 in the PVN, or **b** VGLUT2 and PHAL in the PVN. In **a,** the 5-μm-thick projection image demonstrates that virtually all GLP1-positive varicose fibers and terminals are VGLUT2 positive. The *lower right boxed insert* contains a ×10 epifluorescence image showing intense GLP1-positive axon terminals within the PVN. The *asterisk* in that image illustrates the region where the confocal images were obtained. In **b,** the 5-μm-thick projection image demonstrates colocalization of VGLUT2 within PHAL tracer-labeled fibers originating from the caudal NST. The *upper left boxes* in both panels show 3D rotated views of maximum intensity projections from the *smaller boxed regions. Scale bars* are 5 or 300 μm, as indicated

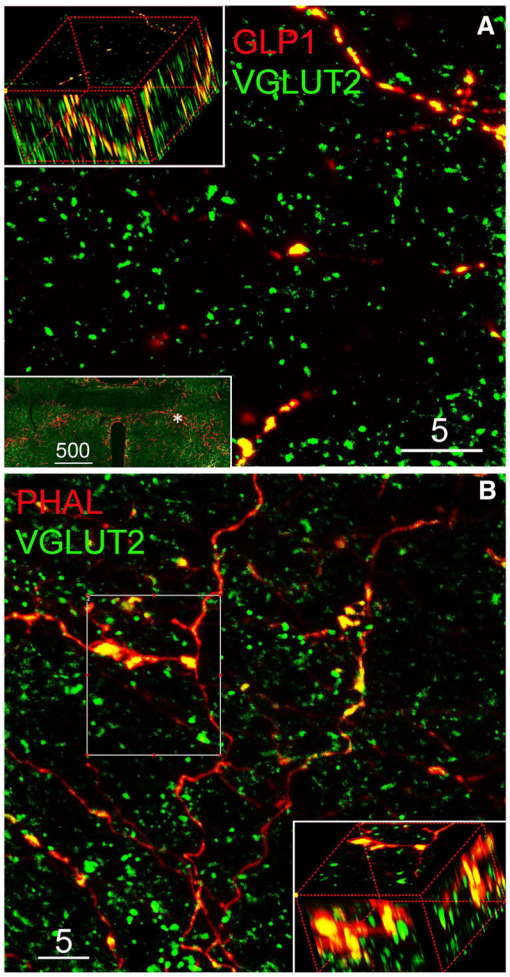

Fig. 3.

Representative confocal images of ICC labeling for VGLUT2, GLP1, and PHAL in the vlBST. **a** 5-μm-thick projection image demonstrates virtually all GLP1-ir varicose axons/buttons are VGLUT2-ir; inserted ×10 epifluorescence image shows the distribution of GLP1-ir axon terminals in the vlBST and the area (*hash*) where confocal image was taken. **b** 5-μm-thick projection image demonstrates the localization of VGLUT2-ir in NST-origin PHAL-ir varicose axon terminals. 3D rotated *inserts* (**a**, **b**) are maximum intensity projection from the regions of interest

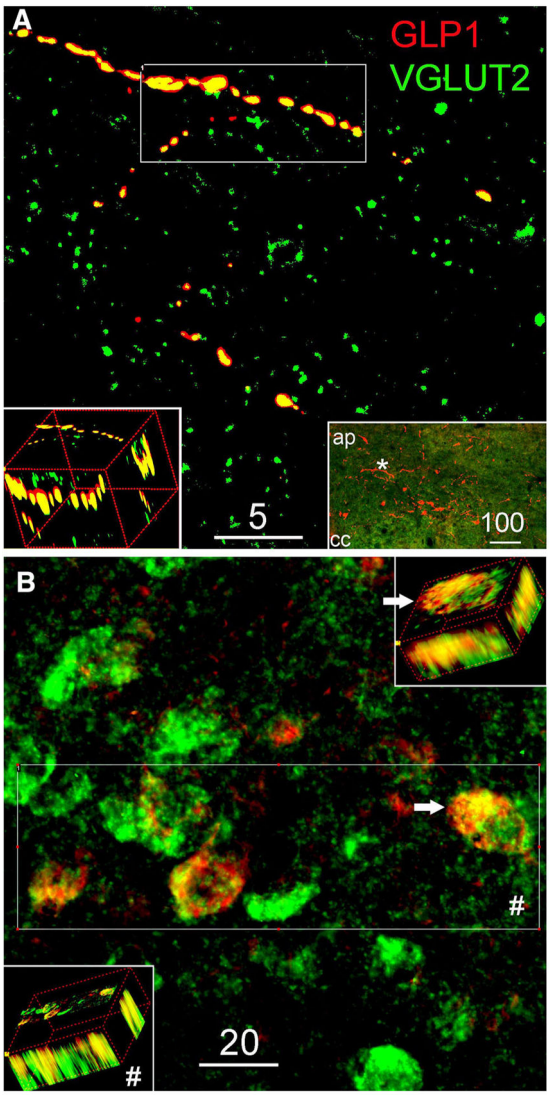

Fig. 4.

Representative confocal images of GLP1 and VGLUT2 in the NST. **a** 5-μm-thick projection image demonstrates the colocalization of GLP1-ir and VGLUT2-ir; 3D rotated *insert* shows the maximum intensity projection from region of interest. Inserted low magnification (×10) epifluorescence image indicates the distribution of GLP1-ir cell bodies and terminals in the NST and the region (*hash*) where the confocal image was taken. **b** 6-μm-thick projection image from combined ISH and IHC labeling demonstrates the localization of GLP1-ir in VLGUT2 mRNA expressing neurons. *Hash*, 3D rotated *insert* shows GLP1-ir in all four VGLUT2 mRNA expressing neurons from the area of interest. *White arrow* provides a detail 3D view from one double-labeled neuron

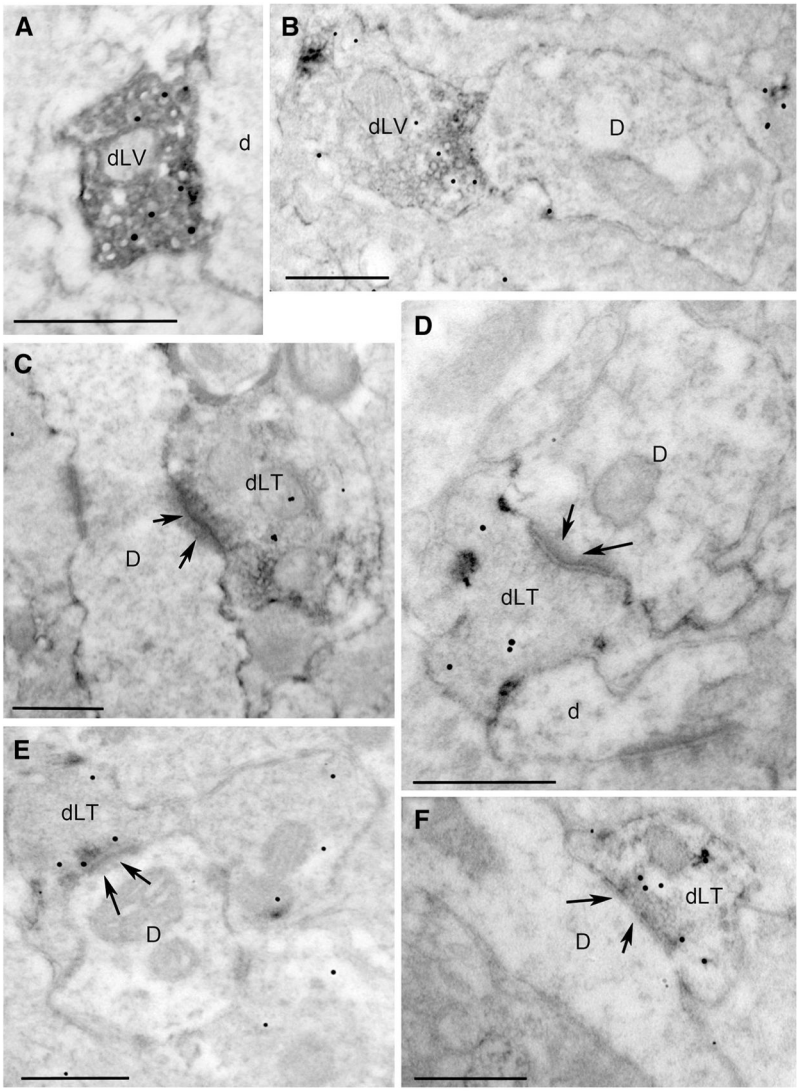

Fig. 5.

Ultrastructural localization of GLP1 immunoperoxidase (floccular electron-dense label) and VGLUT2 immunogold (small particulate label) within the PVN (**a**–**c**) and DMH (**d**–**f**). *D* dendrite, *dLT* double-labeled terminal, *dLV* double-labeled varicosity. *Arrows* point out postsynaptic specializations of asymmetric (i.e., excitatory-type) synapses formed by double-labeled axon terminals onto unlabeled dendrites. All *scale bars* 500 nm